Original Paper

Viscous sintering of non-spherical borosilicate-glass powder

Aldo R. Boccaccini and Gerhard Ondracek

Institut für Gesteinshüttenkunde, Glas, Bio- und Verbundwerkstoffe, Rheinisch-Westfälische Technische Hochschule, Aachen (FRG)

Densification by viscous flow – instead of diffusion – may be investigated by comparing densification rates and flow rates without the effect of external load, if possible. This is why the sintering of a borosilicate-glass powder was investigated using a hot-stage microscope. The samples sintered at 888 K showed shrinkage anisotropy, being the ratio of the axial to the radial shrinkage < 1. The flow rate varies linearly with the densification rate due to anisotropic densification; and the ratio between flow rate and densification rate may be altered by modifying the grade of anisotropy in densification. Scherer's theory has been used to compare experimental and theoretical values and the interdependence between densification rate and density. Deviations are discussed.

Viskoses Sintern von nichtsphärischem Borosilicatglaspulver

Die Verdichtung durch viskoses Fließen – an Stelle von Diffusion – kann beim Sintern von Gläsern durch Vergleich der Verdichtungs- und Fließgeschwindigkeiten ohne Druckanwendung untersucht werden. Für Borosilicatglas wurden diese Untersuchungen im Heiztischmikroskop durchgeführt. Proben, die bei 888 K gesintert wurden, zeigten insofern eine Schrumpfungsanisotropie, als das Verhältnis zwischen der Schrumpfung in axialer Richtung zu derjenigen in radialer Richtung <1 lag. Fließ- und Verdichtungsgeschwindigkeit variieren entsprechend der anisotropen Verdichtung, ihr Verhältnis zueinander variiert mit der Verdichtungsanisotropie. Es wird versucht, durch Vergleich zwischen experimentellen Werten und solchen, die nach der Theorie von Scherer errechnet wurden, den Zusammenhang zwischen Verdichtungsgeschwindigkeit und Dichte zu deuten und Abweichungen zu erläutern.

1. Introduction

Subdividing materials technology in melting and sintering it is traditionally obvious that melting has preference for metals, polymers and glasses, whilst sintering dominates in producing ceramics. High-technology applications, however, such as the vitrification of nuclear wastes, glass filters for biotechnology, porous bioglasses for implants or the sintering of superfine, high-pure glass powders [1], for example, made sintering to be the technology of choice also for glasses [2 and 3]. As frequently observed, also in this case, application feeds back to basic science, since the dominant transport mechanism in glass sintering should not be diffusion but viscous flow. This is due to the amorphous glassy state and in contrast to the common case in sintering crystal ceramics or metals.

Against this background, the sintering of glass has been investigated several times providing results about densification and flow during sintering [4 to 7]. The expression "flow" in this context substitutes "creep", which is frequently used in literature but refers usually to deformation under loading. Most of these works were performed by dilatometric measurements and by application of low uniaxial stresses. The experimental results have been compared with the predictions of theoretical models for viscous sintering, amongst which Scherer's model [8] is one that appears to have a broader applicability as other available models [9], because it assumes a particular geometry that can be applied to the entire densification process. Rahaman et al. [5] found excellent agreement with Scherer's theory by sintering a well-characterized spherical powder of borosilicate glass. On the other hand, experimental results on sintering borosilicate glasses containing rigid inclusions or sintering crushed soda-lime glass powder provided results which showed ambiguity in comparing them with the predictions of Scherer's model [4 and 6]. For example, both the densification rate and the flow viscosity showed a much stronger dependence on density as theory predicts. Moreover, it was found that the shrinkage of the samples was higher in the axial than in the radial direction. This is contrary to previous investigations [10 and 11] on the sintering behaviour of cordierite-type glass powder, where the ratio of the axial to the radial shrinkage was about 0.7 for samples formed by pressing in the axial direction.

Particle alignment produced during compaction and non-uniform binder burnout appear to be the main reasons for the unexpected shrinkage anisotropy observed for the crushed soda-lime glass powder [4]. In order to determine if the strong dependence of the densification rate on density is a general result for

Received March 20, 1991.

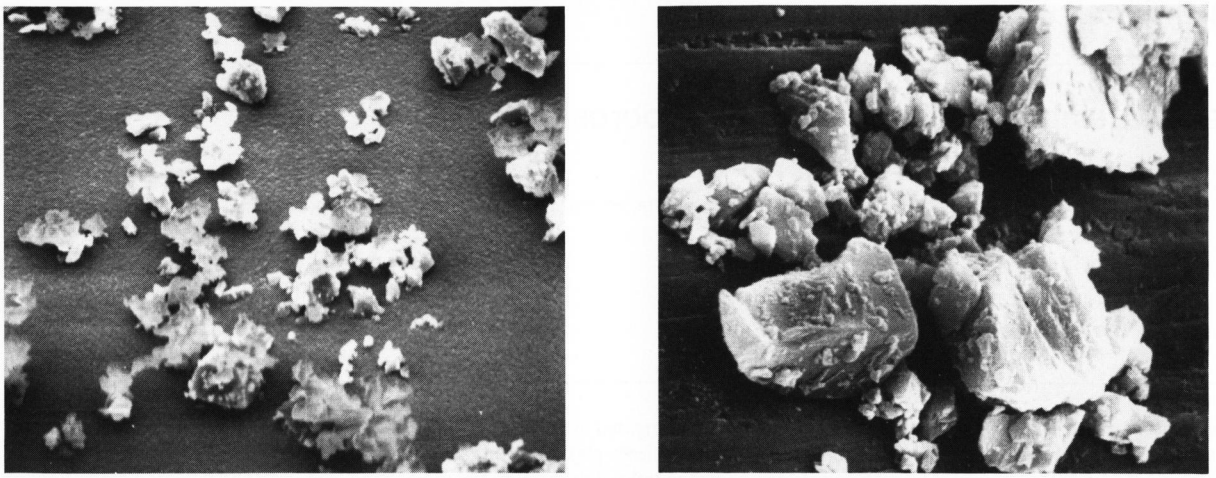

Figures 1a and b. Scanning electron micrographs of the borosilicate-glass powder at a) low and b) high magnifications.

non-spherical glass powders and to investigate the reasons for the unexpected shrinkage anisotropy, in this work the densification and flow rates during sintering of a non-spherical borosilicate-glass powder are investigated. The sintering was performed in a hot-stage microscope, that allowed monitoring of the axial and radial shrinkage without the exertion of any external load. The densification rate obtained from the measurements is compared with the predictions of Scherer's theory.

2. Experimental procedure

A borosilicate-glass powder was used in this work, specially developed for the immobilization of nuclear wastes by sintering [2] and now considered as a potential matrix material for general waste fixation [12]. Based on this work the same glass powder is presently used for studies concerning the sintering of glass-matrix composites containing rigid inclusions [6]. Its mean particle size is 5.5 µm and the theoretical density is 2.57 g/cm^3.

Cylindrical compacts (5 mm in diameter and 5 mm in length) were obtained by uniaxial pressing at room temperature without the addition of any binder. Pressures of 250 MPa were applied to reach relative green densities of 0.59 ± 0.02. Sintering was performed in a hot-stage microscope for 2 h at 888 K in air without the exertion of any external load. This temperature corresponds to the nominal densification range of the borosilicate glass used [2]. After heating the oven to the sintering temperature the compacts were set in quickly, in order to provide isothermal conditions for the whole period of sintering. The axis of the cylindrical samples coincided with the vertical direction. At prechosen time intervals during the sinter process, photographs of the samples were made to measure lengths and diameters and hence to calculate the axial and radial shrinkages.

The mass and dimensions of the pressed and sintered compacts were measured and the geometrical densities determined. Whilst the final density of the sintered pellets was also measured using Archimedes principle, the density as a function of time during sintering was determined from the green density and the measured shrinkage. Scanning electron microscopy was used to investigate the glass powder and the microstructure of the sintered compacts.

3. Data analysis

From the experimental data for the axial and radial shrinkages during sintering the relative density, ϱ, at any time can be found by the expression

$$\varrho = \frac{\varrho_0}{(1 - \Delta R/R_0)^2 (1 - \Delta L/L_0)} \tag{1}$$

where ϱ_0 represents the relative green density and $\Delta R = R_0 - R$, $\Delta L = L_0 - L$. R_0, L_0 are the initial radius and length, respectively, and R, L are the instantaneous radius and length of the sample, respectively.

The data for the axial and radial shrinkages permit also the calculation of the respective shrinkage rates, $\dot{\varepsilon}_z$ and $\dot{\varepsilon}_r$, by the equations

$$\dot{\varepsilon}_z = \frac{\mathrm{d}[\ln (L/L_0)]}{\mathrm{d}t}, \tag{2}$$

$$\dot{\varepsilon}_r = \frac{\mathrm{d}[\ln (R/R_0)]}{\mathrm{d}t}. \tag{3}$$

The flow rate, $\dot{\varepsilon}_f$, and the densification rate, $\dot{\varepsilon}_\varrho$, may be evaluated according to the relations [13]

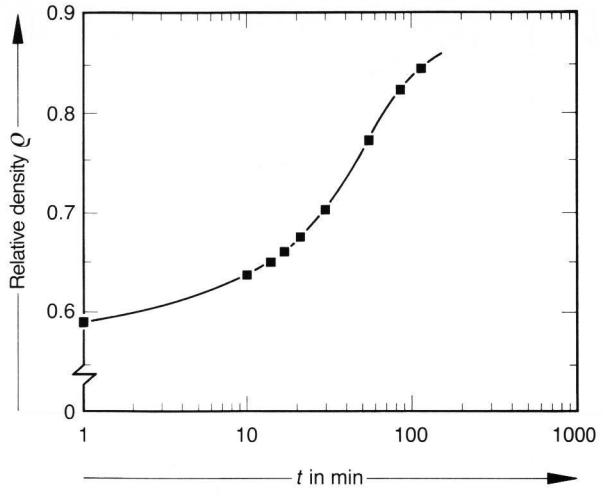

Figure 2. Relative density, ϱ, of borosilicate-glass powder (sintered at 888 K) as a function of sintering time, t.

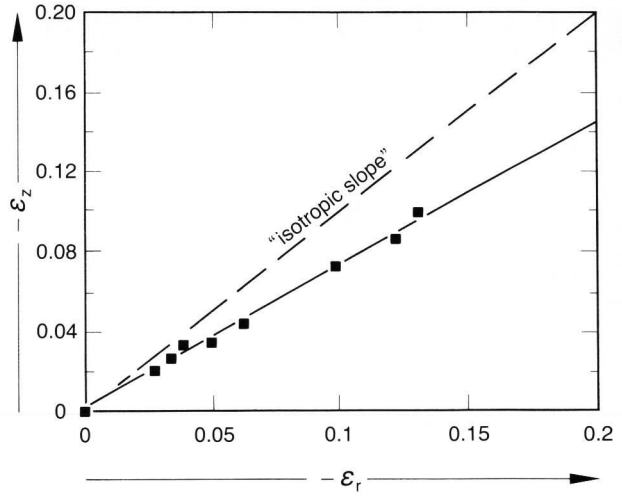

Figure 4. Relation between linear axial shrinkage, ε_z, and linear radial shrinkage, ε_r, of borosilicate-glass powder during sintering.

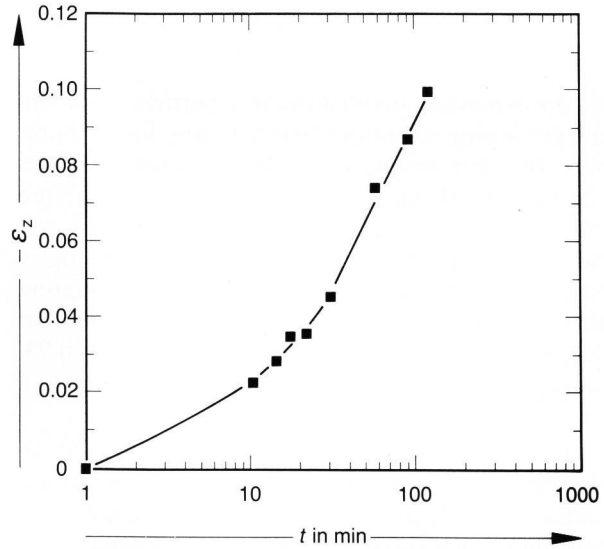

Figure 3. Linear axial shrinkage, ε_z, of borosilicate-glass powder as a function of sintering time, t.

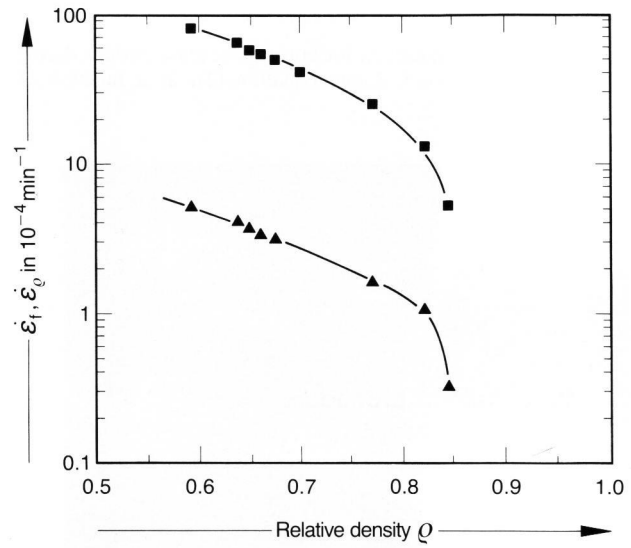

Figure 5. Flow rate, $\dot{\varepsilon}_f$, (▲) and densification rate, $\dot{\varepsilon}_\varrho$, (■) as a function of relative density, ϱ, of borosilicate-glass powder during sintering.

$$\dot{\varepsilon}_f = 2/3\ (\dot{\varepsilon}_z - \dot{\varepsilon}_r)\ , \tag{4}$$

$$\dot{\varepsilon}_\varrho = \dot{\varrho}/\varrho = -\ (\dot{\varepsilon}_z + 2\ \dot{\varepsilon}_r) \tag{5}$$

where $\dot{\varrho}$ is the derivation of the relative density in dependence on the sintering time.

4. Results

Figures 1a and b show scanning electron micrographs of the borosilicate-glass powder used. The non-spherical character of the particles is evident. Figure 2 shows the relative density as a function of sintering time, t. It was calculated using equation (1), the data for radial and axial shrinkage, and the relative green density. The data shown are an average of two runs under the same conditions and have a maximum relative error of 4 %. The final relative density calculated from equation (1) was in good agreement with the values determined using the Archimedes principle.

Figure 3 shows the results for the axial shrinkage, ε_z, versus sintering time and figure 4 shows the results for the axial shrinkage, ε_z, versus the radial shrinkage, ε_r. The densification rate, $\dot{\varepsilon}_\varrho$, was obtained by fitting smooth curves to the data of figure 2 followed by differentiating and application of equation (6)

$$\dot{\varepsilon}_\varrho = \dot{\varrho}/\varrho\ . \tag{6}$$

The results are shown in figure 5 together with the results for the flow rate, $\dot{\varepsilon}_f$. These were obtained by fitting smooth curves to the data of figures 3 and 4 and differentiation according to equation (4). The calculation of the densification rate, $\dot{\varepsilon}_\varrho$, following this procedure and using equation (5) gives results that

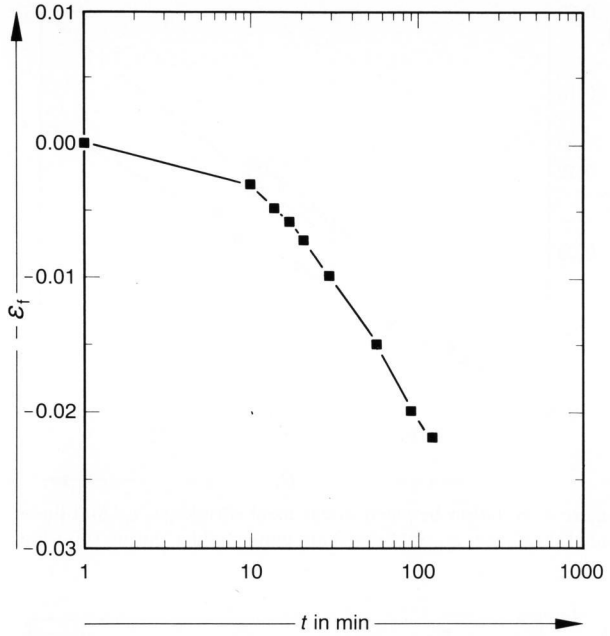

Figure 6. Flow shrinkage, ε_f, for borosilicate-glass powder during sintering (see figures 3, 4 and equation (4)) as a function of sintering time, t.

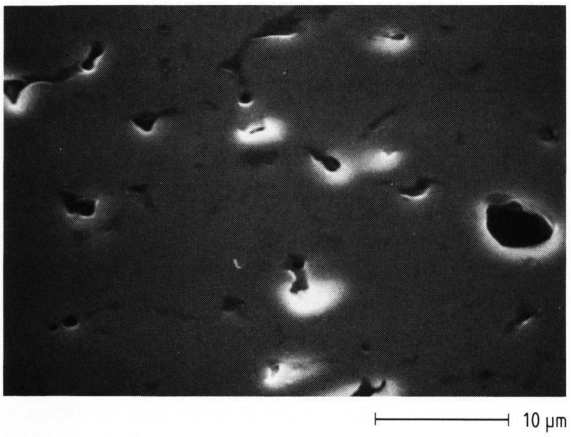

Figure 8. Microstructure of borosilicate-glass powder sintered at 888 K to a relative density of 0.82.

are in excellent agreement with the correspondent values calculated by the density data and equation (6). The results for the flow shrinkage, ε_f, versus sintering time are shown in figure 6.

5. Discussion and conclusions

Figure 4 indicates the anisotropic character of the densification. The shrinkage is lower in the axial than in the radial direction. This result coincides with the results for spherical borosilicate-glass powder [5] and for cordierite-type glass powder [10] but is quite different from the results of the earlier work on crushed soda-lime glass powder [4], in which the samples shrank more in the axial direction.

It confirms that anisotropy in shrinkage is not only influenced by particle shape, but also by other

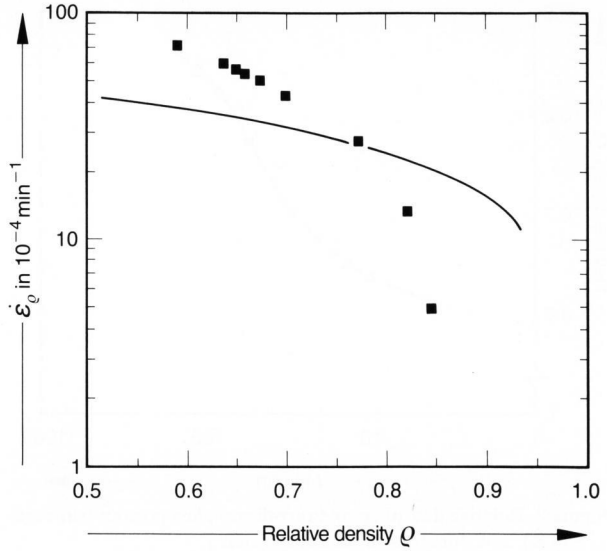

Figure 7. Densification rate, $\dot{\varepsilon}_\varrho$, as a function of relative density, ϱ, for sintered borosilicate-glass powder. (■: experimental values, ——: theoretical values according to Scherer's theory [8].)

factors as particle-size distribution, particle alignment and processing conditions (temperature, binder burnout). In other words: It is a complex set of factors affecting the shrinkage anisotropy, which therefore cannot simply be related to the alteration of one factor, if others change synchronically, effecting – possibly – the shrinkage behaviour in different directions. The slope of the straight line in figure 4 is the strain anisotropy ratio, $\varepsilon_z/\varepsilon_r$, and its value is 0.73, comparable to the shrinkage anisotropy found in previous works [5 and 10].

Following the indication of Rahaman et al. [5], an objective of this paper is to provide experimental results of the densification rate of the non-spherical borosilicate-glass powder as a function of density and to compare these results with the theoretical predictions of Scherer's model [8]. According to this model the densification rate is given by

$$\frac{\dot{\varrho}}{\varrho} = C \frac{(2 - 3.6\, a/l)}{(a/l)^{1/3}\,(1 - 1.2\, a/l)^{2/3}} \tag{7}$$

where C is a constant related to the type of material, a and l, respectively, are the radius and length of the cylinders of the model. The quotient a/l and the relative density are related by the equation

$$\varrho = 3\,\pi\,(a/l)^2 - 8\,\sqrt{2}\,(a/l)^3\,. \tag{8}$$

In figure 7 the experimental results for the densification rate, $\dot{\varepsilon}_\varrho = \dot{\varrho}/\varrho$, are compared with the theoretical predictions. As in the previous work [4] the constant C in equation (7) was arbitrarily chosen to reach an agreement between theory and experiment at a relative density $\varrho = 0.77$. It is seen that the densification rate varies stronger with the density than predicted by Scherer's theory. Since Scherer [14]

has pointed out that the densification rate is very sensitive to the pore-size distribution, the deviation between theoretical and experimental results may be explained by pore-size scattering. A similar explanation was given for the results on crushed soda-lime glass powder [4]. Figure 8 shows the microstructure of a sample with a relative density, ϱ, of 0.82. The distribution in pore sizes is evident.

Putting the ratio between flow rate and densification rate, $\dot{\varepsilon}_f/\dot{\varepsilon}_\varrho$, versus relative density points out (figure 9) that this ratio is almost independent of the relative density, which, according to figure 5, was to be expected. In so far, the linear slope between flow rate and densification rate, as shown in figure 10, is necessary. According to this figure the relation between flow rate and densification rate for borosilicate-glass powder sintered at 888 K may be written as

$$\dot{\varepsilon}_f = 0.07\, \dot{\varrho}/\varrho\ . \tag{9}$$

Rahaman et al. [4] found 0.14 as constant instead of 0.07 studying the sintering of crushed soda-lime glass powder at 878 K. If the temperature does not play a role in affecting this constant ratio because both processes (flow and densification) occur by the same mechanism of viscous flow, the lower flow rate found in this study should be due to a more uniform compact microstructure and therefore lower anisotropy in the shrinkage. And indeed, the ratio between axial and radial shrinkage, $\varepsilon_z/\varepsilon_r$, found in this study is 0.73 while in the case of crushed soda-lime glass powder [4] this ratio was 1.8.Using equations (4 and 5) and considering that the ratio of the axial to the radial shrinkage remains constant during the sinter process ($\varepsilon_z/\varepsilon_r = k$) it is possible to write

$$\frac{\dot{\varepsilon}_f}{\dot{\varepsilon}_\varrho} = \frac{2/3\,|\,k-1\,|}{(2+k)}\ . \tag{10}$$

Figure 11 shows the experimental values for this ratio, $\dot{\varepsilon}_f/\dot{\varepsilon}_\varrho$, from this study and according to Rahaman et al. [4] plotted versus the respective anisotropy ratio, $\varepsilon_z/\varepsilon_r$. Also shown is the curve represented by equation (10). As the interdependence points out, it should be possible to alter the ratio between flow rate and densification rate by variation of the shrinkage anisotropy only, without external load effects. Work is in progress to investigate how the grade of anisotropy of shrinkage can be influenced by particle alignment during the fabrication of the compacts, which finally will end-up in the correlation between densification and powder characteristic on sintering by viscous flow.

*

The work presented here was dominantly assisted by financial support of the Carl-Zeiss-Stiftung, Heidenheim (FRG), and for A.

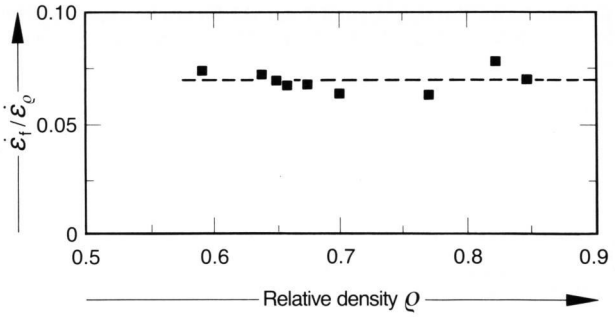

Figure 9. Ratio of flow rate, $\dot{\varepsilon}_f$, to densification rate, $\dot{\varepsilon}_\varrho$, of sintered borosilicate-glass powder as a function of relative density, ϱ. (■: experimental values, – – –: slope fitting.)

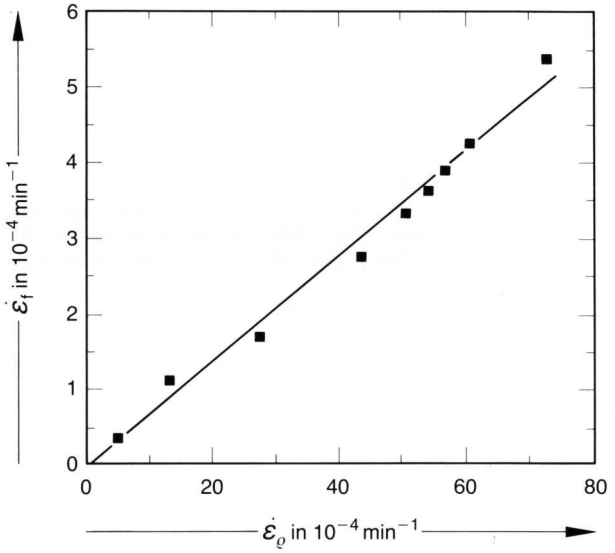

Figure 10. Linear relationship between flow rate, $\dot{\varepsilon}_f$, and densification rate, $\dot{\varepsilon}_\varrho$, for borosilicate-glass powder during sintering.

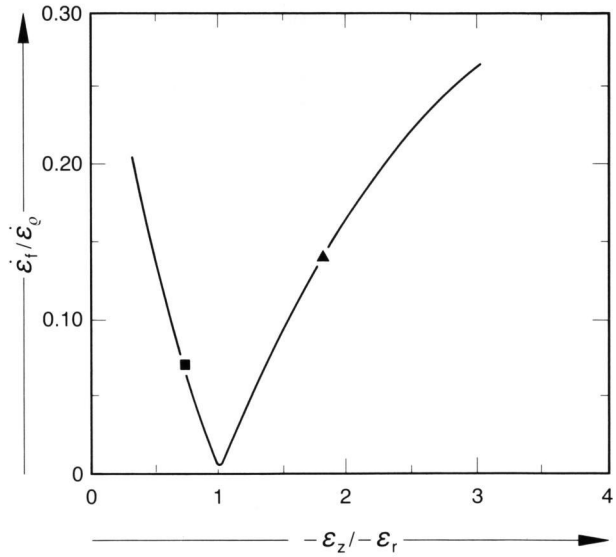

Figure 11. Interdependence of the ratios of flow rate. $\dot{\varepsilon}_f$, to densification rate, $\dot{\varepsilon}_\varrho$, and linear axial shrinkage, ε_z, to linear radial shrinkage, ε_r. (▲: [4], ■: experimental values, ———: theoretical curve according to equation (10).)

R. Boccaccini through a grant from the Deutsche Akademische Austauschdienst (D.A.A.D.), Bonn (FRG). The authors express herewith their grateful appreciation.

6. References

[1] Clasen, R.: Herstellung sehr reiner Kieselgläser durch Sintern submikroskopischer Glasteilchen. Rhein.-Westf. Tech. Hochschule Aachen, Fak. Bergbau, Hüttenwesen u. Geowiss., Habil.-Schrift 1989.

[2] Bauer, C.; Gahlert, S.; Ondracek, G.: Treatment of nuclear waste: Materials technology for producing nuclear waste packages. In: Brookins, D. G. (ed.): The geological disposal of high-level radioactive wastes. Athens: Theophrastus Publ. 1987. p. 207–264.

[3] Gahlert, S.; Ondracek, G.: Sintered glass. In: Lutze, W.; Ewing, R. C. (eds.): Radioactive waste forms for the future. Amsterdam (et al.): North Holland 1988. p. 161–192.

[4] Rahaman, M. N.; De Jonghe, L. C.; Scherer, G. W. et al.: Creep and densification during sintering of glass powder compacts. J. Am. Ceram. Soc. **70** (1987) no. 10, p. 766–774.

[5] Rahaman, M. N.; De Jonghe, L. C.: Sintering of spherical glass powder under a uniaxial stress. J. Am. Ceram. Soc. **73** (1990) no. 3, p. 707–712.

[6] Boccaccini, A. R.; Ondracek, G.: Glass phase containing composed ceramics: The effect of rigid inclusions on the sintering of borosilicate glass. In: Proc. 4th International Otto Schott Colloquium, Friedrich-Schiller-Universität Jena 1990. p. 72–76.

[7] Clasen, R.; Ondracek, G.; Pommer, P. et al.: Herstellung von Kieselgläsern über einen Sinterprozeß von hochdispersen Pulvern: Ausgangsmaterial, Formgebung und Sinterung. Silikattechnik **41** (1990) no. 6, p. 202–206.

[8] Scherer, G. W.; Bachman, D. L.: Sintering of low-density glasses. Pt. 1. Theory. Pt. 2. Experimental study. J. Am. Ceram. Soc. **60** (1977) no. 5–6, p. 236–239; 239–243.

[9] Mackenzie, J. K.; Shuttleworth, R.: A phenomenological theory of sintering. Proc. Phys. Soc. **B 62** (1949) no. 12, p. 833–852.

[10] Giess, E. A.; Fletcher, J. P.; Herron, L. W.: Isothermal sintering of cordierite-type glass powders. J. Am. Ceram. Soc. **67** (1984) no. 8, p. 549–552.

[11] Giess, E. A.; Guerci, C. F.; Walker, G. F. et al.: Isothermal sintering of spheroidized cordierite-type glass powders. J. Am. Ceram. Soc. **68** (1985) no. 12, p. C-328–C-329.

[12] Lutze, W.: Verglasung von toxischen insbesondere hochradioaktiven Abfällen. Rhein.-Westf. Tech. Hochschule Aachen, Fak. Bergbau, Hüttenwesen u. Geowiss. Habil.-Schrift 1992.

[13] Raj, R.: Separation of cavitation-strain and creep-strain during deformation. J. Am. Ceram. Soc. **65** (1982) no. 3, p. C-46.

[14] Scherer, G. W.: Viscous sintering of a bimodal pore-size distribution. J. Am. Ceram. Soc. **67** (1984) no. 11, p. 709–715.

92R0228